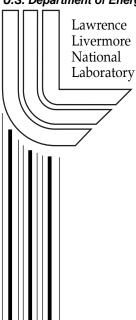
# Hydride Precipitation Crack Propagation in Zircaloy Cladding During a Decreasing Temperature History

R. B. Stout

This article was submitted to the Track-9 Sessions, International Conference on Nuclear Engineering (ICONE), Nice, France, April 8-12, 2001

December 4, 2000





### DISCLAIMER

This document was prepared as an account of work sponsored by an agency of the United States Government. Neither the United States Government nor the University of California nor any of their employees, makes any warranty, express or implied, or assumes any legal liability or responsibility for the accuracy, completeness, or usefulness of any information, apparatus, product, or process disclosed, or represents that its use would not infringe privately owned rights. Reference herein to any specific commercial product, process, or service by trade name, trademark, manufacturer, or otherwise, does not necessarily constitute or imply its endorsement, recommendation, or favoring by the United States Government or the University of California. The views and opinions of authors expressed herein do not necessarily state or reflect those of the United States Government or the University of California, and shall not be used for advertising or product endorsement purposes.

This is a preprint of a paper intended for publication in a journal or proceedings. Since changes may be made before publication, this preprint is made available with the understanding that it will not be cited or reproduced without the permission of the author.

This work was performed under the auspices of the United States Department of Energy by the University of California, Lawrence Livermore National Laboratory under contract No. W-7405-Eng-48.

This report has been reproduced directly from the best available copy.

Available electronically at <a href="http://www.doc.gov/bridge">http://www.doc.gov/bridge</a>
Available for a processing fee to U.S. Department of Energy
And its contractors in paper from
U.S. Department of Energy
Office of Scientific and Technical Information
P.O. Box 62
Oak Ridge, TN 37831-0062

Telephone: (865) 576-8401 Facsimile: (865) 576-5728 E-mail: reports@adonis.osti.gov

Available for the sale to the public from U.S. Department of Commerce National Technical Information Service 5285 Port Royal Road Springfield, VA 22161 Telephone: (800) 553-6847 Facsimile: (703) 605-6900

E-mail: <u>orders@ntis.fedworld.gov</u>
Online ordering: <u>http://www.ntis.gov/ordering.htm</u>

Or
Lawrence Livermore National Laboratory
Technical Information Department's Digital Library
http://www.llnl.gov/tid/Library.html

# HYDRIDE PRECIPITATION CRACK PROPAGATION IN ZIRCALOY CLADDING DURING A DECREASING TEMPERATURE HISTORY

R. B. STOUT, University of California/LLNL

POBox 808(L-201), Livermore, CA 94550. E-mail: stout4@llnl.gov

Key words: Zirhydrides, Crack Propagation, Cladding Failure

### Introduction

An assessment of safety, design, and cost tradeoff issues for short (ten to fifty years) and longer (fifty to hundreds of years) interim dry storage of spent nuclear fuel in Zircaloy rods shall address potential failures of the Zircaloy cladding caused by the precipitation response of zirconium hydride platelets. If such assessment analyses are to be done rigorously, they will be necessarily complex because the precipitation response of zirconium hydride platelets is a stochastic functional of hydrogen concentration, temperature, stress, fabrication defect/texture structures, and flaw sizes of the cladding [2]. Thus, there are, and probably always will be, zirhydride questions to analytically and experimentally resolve concerning the consistency, the completeness, and the certainty of models, data, the initial and the time-dependent boundary conditions. Some resolution of these questions will be required in order to have a defensible preference and tradeoffs decision analysis for assessing risks and consequences of the potential zirhydride induced cladding failures during dry storage time intervals. In the following brief discussion, one of these questions is posed as a consequence of an anomaly described in data reproducibility that was reported in the results of tests for hydrogen induced delayed cracking [3, 4]. The testing anomaly consisted of observing a significant differential in the measurable crack velocities (quasi-steady state at a prescribed load and temperature values) that depended on the approach direction, from above or from below, to the test temperature value. The testing method used was restricted to approaching a prescribed test temperature This anomaly illustrates the known thermodynamic above. non-equilibrium processes in the precipitation kinetics of zirhydride platelets that are dependent on temperature and stress histories. Detailed solubility limits of hydrogen in Zircaloy as a function of temperature, in terms of zirhydride precipitation and zirhydride dissolution solubility curves, were reported recently [5]. In addition, other tests to evaluate the influence of an applied stress state on zirhydride precipitation kinetics have also been recently reported [6].

In the case of a Zircaloy spent fuel rod with typical hydrogen pickup (e.g., 50 to 500 ppm)[7] and with a surface crack/small flaw (e.g., an oxide film through crack), this anomaly in crack velocity testing along with the temperature dependent zirhydride precipitation curves suggests that an annually decreasing temperature history over

interim storage time durations could result in zirhydride induced crack propagation. Most existing models and available test data of zirhydride precipitation near a crack tip are for the evaluation of a critical stress intensity factor at constant temperature. For the thin wall dimensions of Zircaloy cladding (e.g., 0.62 to 0.85 mm)[8], any measurable crack propagation velocity (~10<sup>-8</sup> m/sec) typical means almost instant failure (~ a year) in comparison to dry storage time scales. Hence, a go/nogo design limit given by a critical stress intensity factor is often believed the most appropriate and conservative approach, but may also be too superficial, to evaluate initial cladding flaw sizes for, and/or to promote, an acceptance criterion. However, to improve upon this situation, and to provide estimates for the slow crack propagation velocities where complex mechanisms are often coupled, requires refined test data methods and difficult to derive theoretical models that are based on detailed mechanisms, some of which are inadequately understood. Therefore, the development of a slow crack propagation model will be most useful in cladding design life evaluations for safety, risk, and consequence analyses during interim dry storage. It is for the latter reason that in the following section, two models for zirhydride induced crack propagation velocity are developed for time dependent temperature (decreasing) and stress (increasing) fields, as well as spatial gradients of hydrogen concentration, temperature, and stress. The first model is for quasisteady crack propagation due to zirhydride precipitation and zirhydride growth kinetics. Then, this quasi-steady model will be extended to show the potential for subsequent unstable crack propagation that is primarily stress driven [9]. A detailed discussion and evaluation of the material parameters and cladding failure time predictions will be included in a future paper. The summary section briefly discussed the readily available data that could be used to evaluate some material property parameters of this model and the types of additional tests that could be performed to augment and extend the existing test data.

## **Zirhydride Precipitation Kinetics and Crack Propagation**

The development of the following crack propagation models is based on some uses of and extensions to existing models for hydride platelet statistical mechanics, hydride platelet precipitation and growth kinetics, hydride dependent deformations and induced stresses, and hydride dependent thermodynamics [2]. In this deformation and thermodynamic model development, a hydride surface energy functional was incorporated, the thermodynamic surface energy term has been ignored in previous model developments, as well as explanation discussions of hysteresis responses in solubility data [5]. Here, the platelet growth kinetics of reference [2] will be extended as the primary topic of this crack propagation model. Nonetheless, in the following, each of the above topics will be discussed in the context of describing and deriving an idealized model for small flaw crack propagation due to a single generic zirhydride platelet that precipitates and growths in front of the crack. A key assumption is that the hydride platelet growth in front of the crack is the mechanical equivalent to inserting a wedge to maintain a quasisteady opening and stress state moving with the leading edge of the growing hydride platelet. Idealistically, this also implies that the zirhydride platelet grows in the thickness direction until it attains a local compressive state for the additive effects of both external and locally internal stresses. Eadie and Ellyin [10] assumed these concepts of a compressive hydride stress state in their analysis for the stress effects

due to a hydride platelet near the crack tip. <u>This key assumption</u>, as used here, will also imply that the effective crack tip in the cladding thickness direction is located at the leading edge of the hydride platelet. Therefore, for purposes of this model development, the growth of the crack tip hydride platelet is effectively the same as the growth of the crack, which is a conservative criterion for evaluating spent fuel cladding failure rates.

The mechanism for evolution from a tensile stress state typical at a crack tip to a compressive stress state of the growing hydride platelet is the volume increase of the zirhydride phase relative to that of the Zircaloy. This depends somewhat on the zirhydride phase and stoichiometric composition of the platelet. Typically, the transformation of a Zr (alpha  $\sim 6.50$ g/cc) phase to a ZrH [x=1.59] (delta  $\sim 5.65$ g/cc) phase or to a ZrH [x=1] (gamma ~5.84g/cc) phase has an increase of ~ 15% and ~ 11% volume strain, respectively [11]. Considering these significant volume strains as inducing an isotropic strain tensor for a kinematic metric of the deformation state. then each of the diagonal components of the strain tensor has a nominal corresponding value of ~ 5% and ~ 3.6%. Both of these strain values are very large relative to the typical 0.2% unjaxial strain limits defined as associated classical phenomenological values at which plastic and/or non-recoverable deformations are, by convention, agreed to have occurred. This order of magnitude in mismatch strain components across a zirhydride platelet boundary would be more than sufficient to initiate dislocation dependent deformations in a neighborhood of a platelet's exterior edge surface. In fact, dislocation dependent deformations are necessary to satisfy idealized zirhydride to zirconium lattice phase interface compatibility of displacement conditions without local microcrack kinetics [12].

In reference [2], the analytical approach for hydride precipitation kinetics was in terms of a probabilistic hydride density function, h(x,t,q)dQ(q)dV(x), for the number of hydride platelets of species  $\mathbf{q}$  in a dQ( $\mathbf{q}$ ) volume of hydride species space for point  $\mathbf{x}$ in a spatial volume  $dV(\mathbf{x})$  at time t. For spatially and species dense sets of hydride platelets per unit volume, a quasi-continuous function space  $\{h(x,t,q)\}$  for the probable density of hydride platelets was assumed to exist in order to develop a kinetics model for hydride precipitation and orientation rates. A hydride platelet species was dimensionally characterized by six physical attributes, thereby defining a six vector **q** species space, to describe current platelet thickness, vector (**c**) and platelet size, two vectors (a,b), and to describe the time rate of change in platelet thickness and platelet size there are three corresponding rates with respect to time vectors, (**c,a,b**). Using this notation, species **q** is identified as a six vector point (c,a,b, c,a,b) in a hydride species space Q(q). The plate area size, area rate, and area orientation metrics for a isolated hydride platelet are given by vector crossproducts of species vectors (a,b, a,b), which in Cartesian tensor notation are  $\mathbf{e}_{imn}\mathbf{a}_{m}\mathbf{b}_{n}$  for the platelet area vector, and  $\mathbf{e}_{imn}\mathbf{a}_{m}\mathbf{b}_{n}$  and  $\mathbf{e}_{imn}\mathbf{a}_{m}\mathbf{b}_{n}$  for platelet area rate vectors. Here, the Cartesian tensor e<sub>imn</sub> is the third order, isotropic (also called the alternating) tensor. The volume and thickness volume growth rate of a platelet are denoted by  $c_i e_{imn} a_m b_n$  and  $c_i e_{imn} a_m b_n$ , respectively, and the two areal volume growth rates are  $c_i e_{imn} a_m b_n$  and  $c_i e_{imn} a_m b_n$ .

In the case of crack growth due to the precipitation of a single zirhydride platelet at an existing sharp, but small flaw crack, the assumption of a spatially

quasi-continuous function space  $\{h(x,t,q)\}$  for the probable density of hydride platelets will not be applicable, as the main concern is the growth rate of a single hydride platelet located at the crack tip. In spent fuel cladding, a small flaw crack on the outer rod surface can be realized by radial surface cracks through the thin zir-oxide film on the Zircaloy cladding. These surface cracks through the non-ductile oxide film appear if the Zircaloy circumferential creep attains about 0.1 to 0.2 percent strain. A function space  $\{h(x,t,q)\}$  for the probable density of hydride platelets will still exist and is described spatially in terms of a generalized function space containing Dirac delta functions. Thus, the spatial location of this platelet is specified as fixed at a generic crack tip. And, the primary model development for crack growth rate will be a description of how a single species q, that precipitated at a generic crack tip, evolves as a six vector point  $(\mathbf{c}, \mathbf{a}, \mathbf{b}, \mathbf{c}, \mathbf{a}, \mathbf{b})$  in a hydride species space  $Q(\mathbf{q})$ . For this particular case, the six vector evolution problem becomes greatly simplified to a single function evolution problem as the following assumptions can be made to obtain an approximate, but physically realistic geometric model growth of a single hydride. First, fix a Cartesian coordinate system  $(x_1, x_2, x_3)$  such that the plane  $(x_1, x_2)$ is in the mid-plane of the oxide film crack with the (x2) axis in the radial direction of crack growth path through the cladding. Then, the (x<sub>1</sub>) axis is parallel to the length axis of the Zircaloy rod, and the (x<sub>3</sub>) axis is perpendicular to the crack mid-plane and is also tangential to the circumferential direction of the Zircaloy rod. Then, for a constant thickness hydride platelet species of unit axial length in the plane of the crack, the species vector attributes (c,a,b, c,a,b) reduce to three vector components for platelet size and one vector component for platelet growth rate, denoted as  $(c_3,a_1,b_2,0,0,b_2)$ . In terms of hydride species functions, the vector component  $b_2$  is the time rate of change for the hydride growth dimensional vector  $\mathbf{b}_2$ , ahead of the original crack tip. Thus, there is only one independent attribute function. The rate of volume increase for this hydride platelet per unit length a<sub>1</sub> is given in general by

$$\Delta V/\Delta t = c_i e_{imn} a_m b_n \qquad \text{and by} \qquad (1)$$

$$= c_3 e_{312} a_1 b_2 \tag{2}$$

when written in terms of the non-zero component vectors of the hydride species at the crack tip. This volume rate of change is directly related to the number rate of hydrogen atoms reacting to form the zirhydride phase of the platelet. A zirhydride phase ZrH(x) is formed by the chemical reaction

$$Zr + xH \Leftrightarrow ZrH_x$$
 (3)

Thus, each of the original Zr atoms of the hydride platelet will have reacted with xZr number of hydrogen atoms during the phase formation of a zirhydride platelet. Similarly, a unit rate with respect to time of Zr atoms per second will have to react with xZr hydrogen atoms per second. This means that if the matrix concentration of hydrogen (atoms/cc), [H], is changing at rate  $\Delta$ [H] /  $\Delta$ t, then the above reaction is progressing at a rate limited by  $\Delta$ [H/x] /  $\Delta$ t. Then from Eq (2) and Eq (3), the rate, in number of Zr atoms per second, that is reacting during the edge growth, at rate  $b_2$ , of the platelet is equal to a supply rate of hydrogen atoms from the rate of depletion of

the available differential atomic hydrogen concentration  $[\delta H(\mathbf{x},t,\mathbf{v})]$  in a local, but somewhat arbitrary, Zr matrix neighborhood volume  $\delta V$  of the platelet's edge;

$$[Zr] \mathbf{c}_3 \mathbf{e}_{312} \mathbf{a}_1 \mathbf{b}_2 = \int \int \Delta[\delta H(\mathbf{x}, t, \mathbf{v})/x] / \Delta t \, d\delta V \, d\mathbf{v}$$
 (4)

where [Zr] is  $\sim 4.29 \times 10^{22}$  atoms/cc, the number of Zr atoms per cubic centimeter ([11] found by multiplying Avogadro's number, 6.023x10<sup>23</sup>, times the Zr density, 6.5g/cc, and divided by the Zr grams per gram mole, 91.2), and v is the diffusional velocity of hydrogen atoms relative to the velocity of Zr atoms, which are for practical purposes spatially fixed. In the local Zr matrix, the available differential atomic hydrogen concentration  $[\delta H(\mathbf{x},t,\mathbf{v})]$  is equal to the matrix hydrogen concentration,  $[H(\mathbf{x},t,\mathbf{v})]$ , minus the precipitation solubility hydrogen concentration at thermodynamic equilibrium,  $[H_{eq}(\mathbf{x},t)]$ . For conditions of constant stress and temperature, spatially and time-wise, and in the presence of hydride precipitates, the matrix concentration of hydrogen will become, in time, equal to the precipitation solubility hydrogen concentration at thermodynamic equilibrium. And for these given conditions, the differential atomic hydrogen concentration  $[\delta H(\mathbf{x},t,\mathbf{v})]$  and its rate of change with respect to time would be zero. However, for non-equilibrium thermodynamic conditions, the differential atomic hydrogen concentration  $[\delta H(\mathbf{x},t,\mathbf{v})]$  and its rate of change are nonzero as matrix hydrogen may be available because of a flux of hydrogen atoms (non-zero {v} diffusional velocity domain) or because the precipitation solubility hydrogen concentration at thermodynamic equilibrium.  $[H_{eq}(\mathbf{x},t)]$  is changing as a consequence of spatial and time-wise temperature and/or stress changes. These latter rate changes in precipitation solubility hydrogen concentration,  $[H_{eq}(\mathbf{x},t)]$ , provide a source-like rate term of hydrogen atoms to the differential atomic hydrogen concentration  $[\delta H(\mathbf{x},t,\mathbf{v})]$  that are available for the hydride platelet growth reaction at the rate  $b_2$  as given in Eq. (4). Using this discussion, Eq. (4) can be written as

$$[Zr] \mathbf{c_3} \mathbf{e_{312}} \mathbf{a_1} \mathbf{b_2} = \int \int \Delta \left( [H(\mathbf{x}, t, \mathbf{v}) / x] - [H_{eq}(\mathbf{x}, t) / x] \right) / \Delta t \, d\delta V \, d\mathbf{v}$$
 (5)

Using the balance equation for conservation of matrix hydrogen concentration (the time rate of change of hydrogen concentration in a volume plus the surface flux of hydrogen through the surface of that volume must equal zero), the integral of Eq (5) can be written as a surface integral on  $\{\delta v\}$  of volume domain  $\{\delta V\}$  for the matrix function  $[H(\mathbf{x},t,\mathbf{v})/x]$  minus the volume integral of the rate of function  $[H_{eq}(\mathbf{x},t)/x]$ ;

$$[Zr] \mathbf{c_3} \mathbf{e_{312}} \mathbf{a_1} \mathbf{b_2} = \int_{\{\delta V\}} \int_{\{\mathbf{v}\}} \Delta \left( [H(\mathbf{x}, \mathbf{t}, \mathbf{v}) / x] - [H_{eq}(\mathbf{x}, \mathbf{t}) / x] \right) / \Delta t \, d\delta V \, d\mathbf{v}$$
 (6)

$$= - \int_{\{\delta v\}} \int_{\{v\}} \left( \mathbf{v} \cdot \mathbf{n} \left[ \mathbf{H}(\mathbf{x}, t, \mathbf{v}) / x \right] \right) d\delta v d\mathbf{v} - \int_{\{\delta V\}} \int_{\{v\}} \Delta \left[ \mathbf{H}_{eq}(\mathbf{x}, t) / x \right] / \Delta t d\delta V d\mathbf{v}$$
 (7)

where the first surface integral with  $\mathbf{v}_*\mathbf{n}$ , for the diffusional velocity of matrix hydrogen atoms through surface  $\delta v$ , provides a flux of available hydrogen to the growing edge of the platelet and the second volume integral provides available hydrogen from a volume  $\delta V$  as the matrix hydrogen concentration follows any rate changes in the precipitation solubility hydrogen concentration as temperature and stress states change over time. Since the volume  $\{\delta V\}$  and its associated surface  $\{\delta v\}$  are somewhat arbitrary, they can be chosen such that a mechanistic, but idealistic,

model of the diffusional hydrogen flux to the platelet's growth edge is quantified. To do this, consider first a surface  $\{\delta v\}$  which contains a surface subset that is contiguous to the platelet's growth edge, which from Eq (6) is the area vector A<sub>2</sub> given by the vector cross product of  $\mathbf{c}_3\mathbf{e}_{312}\mathbf{a}_1$ . These vector areas can be written as scalar areas by using the local unit normal vector of the surface,  $\mathbf{n_2}$ , to get scalar area terms  $A_2n_2$  or equivalently,  $c_3e_{312}a_1n_2$ . Mathematically, the surface  $A_2n_2$ between the hydride phase and the adjacent zir-metal can be thought of as an effective area-sink for an incoming flux of hydrogen atoms. And along this area-sink the hydrogen atoms are stopped in that their diffusional velocity,  $v \cdot \mathbf{n}$ , becomes zero as the hydrogen chemically reacts with zir-metal atoms to form additional molecules of zirhydride, in a mathematical model representational sense, on surface  $A_2n_2$ . Therefore, for this idealized platelet growth surface  $A_2n_2$  which is a subset of the total surface  $\{\delta v\}$ , the integral flux of hydrogen in Eq. (7) is equal to zero, as all of the hydrogen atoms coming through the complementary surface subset  $\{\delta v - \mathbf{A}_2 \mathbf{n}_2\}$  are essentially deposited as zirhydride at the A<sub>2</sub>n<sub>2</sub> surface. This "essentially" deposited is absolute for the case of time-wise constant temperature and stress fields and when there are no other hydride platelets in volume  $\{\delta V\}$  as the second integral over volume  $\{\delta V\}$  has a zero integrand under these conditions. Then, for this special case, consider the volume point set  $\{\delta V\}$  slightly modified such that the surface  $\{\delta v\}$  is contoured to be within a small, in the math sense, neighborhood  $A_2n_2$  outside of the zirhydride platelet's edge and is now a point subset in the zir-metal which is denoted as  $A_2n_2$ , and elsewhere surface  $\{\delta v\}$  is unchanged. Based on this discussion, the flux of hydrogen through the newly contoured surface,  $A_2n_2$ , now provides the hydrogen atoms to the adjacent neighboring area-sink surface  $A_2n_2$  of the hydride platelet. Then from the first integral of Eq (7), and this case of constant temperature and stress fields, the following integrals are equal for any otherwise arbitrary volume set  $\{\delta V\}$ :

$$\int_{\{\delta v\}} \int_{\{v\}} (\mathbf{v} \cdot \mathbf{n} \left[ \mathbf{H}(\mathbf{x}, t, \mathbf{v}) / x \right]) \, d\delta v \, d\mathbf{v} = \int_{\{\delta v - \mathbf{A} \cdot \mathbf{2} \cdot \mathbf{n}^2\}} \int_{\{v\}} (\mathbf{v} \cdot \mathbf{n} \left[ \mathbf{H}(\mathbf{x}, t, \mathbf{v}) / x \right]) \, d\delta v \, d\mathbf{v}$$

$$= - \int_{\{\underline{\mathbf{A}} \cdot \mathbf{2} \cdot \mathbf{n}^2\}} \int_{\{v\}} (\mathbf{v} \cdot \mathbf{n} \left[ \mathbf{H}(\mathbf{x}, t, \mathbf{v}) / x \right]) \, d\delta v \, d\mathbf{v} \quad (8)$$

Before rewriting Eq (7) with this latter integral of Eq (8), consider adding the following restrictions on the arbitrariness of the choices for volume subset  $\{\delta V\}$  such that, as above, this restricted subset  $\{\delta V\}$  does not contain any other hydride platelets to which hydrogen can diffuse to or from except the isolated crack tip hydride. As such, there exists still a considerable degree of arbitrariness in the volume size of the subsets  $\{\delta V\}$ . This restricted subset  $\{\delta V\}$  of volume choices requires each to contain the contoured surface,  $\underline{A}_2 n_2$ , thus each is in a local neighborhood contiguous to the hydride surface  $A_2n_2$ ; and requires each to be in the domain of hydrogen diffusion influence of only the isolated hydride platelet at the crack tip. The physical significance of this restricted subset of volume choices near the crack tip hydride means that there is a range of volume sizes, each of which hydrogen can diffuse into through surface,  $\{\delta v - \mathbf{A_2} \mathbf{n_2} \}$ , on its pathway to the hydride platelet through surface  $A_2n_2$  and that any available matrix hydrogen concentration rate due to changes in thermodynamic solubility limits evaluated at the local state of temperature and stress can be additive as indicated in the second integral of Eq (7). Note that these changes in thermodynamic solubility limits are to be occurring at small rates of change in the local temperature and stress states such that local thermodynamic equilibrium

between the matrix hydrogen  $[H(\mathbf{x},t,\mathbf{v})]$  and the solubility limit hydrogen  $[H_{eq}(\mathbf{x},t)]$  concentrations is, to a practical approximation, maintained. This equilibrium should be reasonably maintained for temperature decreases typically expected during interim time scales and during slow rates of hydride platelet growth before any crack propagation instability occurs.

Then from Eqs (6), (7), and (8), and some remarks from the above discussion, the velocity attribute  $b_2n_2$  for the platelet growth of the generic crack tip hydride is:

$$b_2 n_2 = ([Zr] \mathbf{A}_2 n_2)^{-1} (\int_{\{\underline{\mathbf{A}}_2 n_2\}} (\Lambda_* \mathbf{n} [H(\mathbf{x}, t, \Lambda) / x]) d\delta v - \int_{\{\delta V\}} \Delta [H_{eq}(\mathbf{x}, t) / x] / \Delta t d\delta V)$$
(9)

where integration over the diffusional velocity domain  $\{v\}$  is replaced by an integral average,  $\Lambda_* n$  [H( $\mathbf{x},t,\Lambda$ )], which defines a net diffusion flux function for hydrogen transport to the platelet at average velocity  $\Lambda_* n$  relative to the zir-metal lattice. The mean theorem of integral calculus can be applied to Eq (9) to derive approximations for surface and volume hydrogen contributions to the platelet growth velocity:

$$\boldsymbol{b}_2 \mathbf{n}_2 = ([Zr] \mathbf{A}_2 \mathbf{n}_2)^{-1} ((\Lambda_* \mathbf{n} [H(\mathbf{x}_A, t, \Lambda) / x]) \underline{\mathbf{A}}_2 \mathbf{n}_2 - \Delta [H_{eq}(\mathbf{x}_V, t) / x] / \Delta t \delta V)$$
(10)

where the integrand of the surface integral is evaluated at point  $x_A$  on area  $\underline{A}_2n_2$  and the integrand of the volume integral is evaluated at point  $x_V$  in volume  $\delta V$ . Eq (10) indicates that the crack tip hydride platelet will grow at a rate proportional to the diffusional flux of hydrogen to the platelet's edge and proportional to the negative rate of change in the equilibrium solubility limit. In linear thermodynamic diffusion theory, the diffusional flux of hydrogen in zir-metal depends on the gradient of its chemical potential, which is dependent on the hydrogen concentration, the temperature, and the stress. The phenomenological expression for this coupled diffusion in terms of gradients of the hydrogen concentration, the temperature, and the stress [13, 14, 15, 16, 6] is complex and there are some potential inconsistency because of the existence and possible influence of dislocations on both diffusion and solubility limits; but for purposes here, the following will be used:

$$\Lambda_{\mathbf{i}}[\mathsf{H}(\mathbf{x},t,\Lambda)] = -\mathsf{D}\partial_{\mathbf{i}}\mathsf{H}(\mathsf{x}_{\mathbf{i}},t) - \mathsf{D}\mathsf{H}(\mathsf{x}_{\mathbf{i}},t)\mathsf{Q}^{*}/\mathsf{RT}^{2}\partial_{\mathbf{i}}\mathsf{T}(\mathsf{x}_{\mathbf{i}},t) + \mathsf{D}\mathsf{H}(\mathsf{x}_{\mathbf{i}},t)\gamma_{\,\,\mathrm{mn}}^{*}/\mathsf{RT}\partial_{\mathbf{i}}\sigma_{\mathrm{mn}}(\mathsf{x}_{\mathbf{i}},t) \tag{11}$$

In Eq (11), D is the classical diffusion function material property,  $\partial_i$  H(x<sub>i</sub>,t) is the spatial gradient of the matrix hydrogen concentration field, Q is a heat energy of transport material property common to coupled mass and temperature diffusion problems, R is the gas constant,  $\partial_i T(x_i,t)$  is the spatial gradient of the temperature field,  $\gamma_{mn}$  is a strain tensor material property for an incremental volume and shear strain induced by the addition of hydrogen atoms into a zir-metal lattice and is used to describe a stress-strain energy of transport that is not so common in coupled mass and stress diffusion problems, and finally,  $\partial_i \sigma_{mn}(x_i,t)$  is the spatial gradient of the Cauchy stress tensor field. Normally, the stress-strain energy term is reduced to an isotropic, incremental volume dependence only, and the stress tensor gradient dependence on diffusion is represented as a scalar pressure gradient dependence. There exist some differences, and confusion, in the identification of the stress state  $\sigma_{mn}(x_i,t)$  that is to be substituted in to Eq (11). The use of only the "applied stress" from the solution to the applied traction and/or displacement boundary condition

problem is only a partial contribution to the local state of stress in a material body. As both the hydride precipitate and dislocation densities also create additional states of intrinsic stress, and since the latter two stress states evolve as the hydride and dislocation densities evolve, a limited "applied stress" coupling in Eq (11) would not mechanistically be adequate to fully describe these latter influences. Given these qualifications, and as well known, Eq (11) implies that hydrogen is transported down hydrogen and temperature gradients, and is transported up a stress gradient. The effects of hydrogen and stress gradients have been modeled [1, 3, 4]. Using these stress dependent results as guidance, the above expression of Eq (11) for hydrogen flux, when substituted into Eq (10), provides the additional temperature gradient dependence on hydrogen transport to the hydride platelet at the crack tip.

For cases of radial and/or axial temperature dependence in spent fuel Zircaloy cladding such that the outer surface crack tip is spatially at the lowest temperature, then the temperature gradient will augment any existing hydrogen transport caused by the concentration and stress gradients. An assessment of this effect can, in an engineering sense, be evaluated with this extended model of temperature dependent hydrogen transport. Hence, the implications are, for purposes of evaluating cladding failures due to hydride driven crack propagation in interim dry storage, that existing concentration-stress models are potentially non-conservative.

In addition to the above discussion for local diffusive transport through the volume subset  $\{\delta V\}$ , and across surface  $\underline{A}_2n_2$  to the platelet's growth edge, the rate of change in the equilibrium solubility limit also provides hydrogen for hydride growth during a decreasing temperature history. There are several temperature dependent expressions available for the hydrogen precipitation solubility limit in zir-metal, all recent ones being similar in that the primary function dependence is Arrhenius [5, 6]. However, the stress dependence is more complex in functionality because the applied state of stress, from an external prescribed load/traction and/or displacement boundary condition is significantly modified by the localized volume changes induced by the hydride platelets. The most recently available representation of a stress dependence on solubility and associated data [6] has provided the following expression for the equilibrium hydrogen concentration function  $[H_{eq}(\mathbf{x},t)]$  given in terms of an Arrhenius temperature term plus a scalar stress work term, and for modeling purposes here will be used:

$$[H_{eq}(\mathbf{x},t)] = [H_{eqo}] \exp(-Q/RT(\mathbf{x},t) - \Delta \gamma_H \sigma_H(\mathbf{x},t)/RT(\mathbf{x},t))$$
(12)

In Eq (12), the equilibrium solubility limit  $[H_{eq}(\boldsymbol{x},t)]$  is seen to be an implicit function of the temperature  $T(\boldsymbol{x},t)$  and stress scalar  $\sigma_H(\boldsymbol{x},t)$  (here  $\sigma_H(\boldsymbol{x},t) = (\sigma_{11}(x_i,t) + \sigma_{22}(x_i,t) + \sigma_{33}(x_i,t))/3)$  fields, and the material property parameters of an empirical atomic concentration  $[H_{eqo}]$ , a positive activation energy Q, and a positive partial molar atomic volume strain  $\Delta \gamma_H$  as atoms of hydrogen transforms from an interstitial zir-metal lattice sites into zirhydride phase hydrogen lattice sites. Looking back at Eq (10), the hydride growth rate functional will require the total time derivative of the

equilibrium hydrogen concentration at point  $\mathbf{x} = \mathbf{x}_{\mathbf{V}}$  in the platelet's neighborhood volume  $\delta \mathbf{V}$ , which from Eq (12) is:

$$d[H_{eq}(\mathbf{x}_{V},t)]/dt = [[H_{eqo}]\exp(-Q/RT(\mathbf{x}_{V},t) - \Delta \gamma_{H}\sigma_{H}(\mathbf{x}_{V},t)/RT(\mathbf{x}_{V},t))] [(+Q/RT^{2}(\mathbf{x}_{V},t) + \Delta \gamma_{H}\sigma_{H}(\mathbf{x}_{V},t)/RT^{2}(\mathbf{x}_{V},t))(dT(\mathbf{x}_{V},t)/dt) - \Delta \gamma_{H}(d\sigma_{H}(\mathbf{x}_{V},t)/dt) / RT(\mathbf{x}_{V},t)]$$
(13)

From Eq (13), it is seen that for decreasing temperatures, i.e., rate of temperature is negative, which is typical for interim spent fuel storage over long time periods, the equilibrium hydrogen concentration decreases and its negative rate provides positive net hydrogen to the hydride platelet's growth as per Eq (10). This is an explanation of the testing anomaly in temperature described in references [3,4]. In addition to the temperature rate dependence, Eq (13) also has a stress rate dependence, which implies that at increase in scalar "tensile" stress will cause a decrease in the equilibrium hydrogen concentration. Thus, any positive rate in local scalar "tensile" stress will provide positive net hydrogen to the hydride platelet's growth as per Eq (10). The above discussion is for a quasi-steady, model of slow hydride growth at crack tip, and because of the original key assumption, an equivalent effective crack propagation velocity. For a quasi-steady model, the rates in temperature and stress are assumed to be monotonic in direction (negative and positive signed, respectively), if not in actual values. Some of the features observed in the careful and high quality crack-hydride growth tests performed by Shek et al. [17] are potentially describable by this model. If the rates of temperature and/or stress are not monotonic in direction, for example seasonal temperature boundary conditions could cause positive and negative rates (daily cyclic variations may be lost in heat capacity inertia) in an interim spent fuel storage facility, then additional considerations should be given to both the precipitation and dissolution solubility curves described in reference [5]. Future extensions to the above model are possible that would address some issues and concerns of a restricted subset of cyclic temperature histories, but the model requirements at small rates of temperature change would have to be investigated and be validated by additional testing.

The above model development considered quasi-steady hydride-crack growth due to diffusive and solubility limited rate hydrogen availability to the edge of a crack tip hydride platelet. For thin walled cladding, there comes a time at which the state of stress, and its time rate of change as well as it spatial gradient, are significantly influenced by the length increase in the original crack length relative to the remaining cladding thickness. This effect can be evaluated by different, but similar approaches. In reference [9], an analysis was completed for a thermodynamic condition of crack propagation initiation, and a subsequent kinematic expression for crack propagation, subject to satisfying brittle fracture requirements at the crack tip. The brittle fracture requirement was stated in terms of having the thermodynamic potential (somewhat similar to the classical thermodynamic chemical potential) for crack kinetics constant during crack propagation. Using this concept, but applying it to a moving stress state

at moving point  $\mathbf{x} = \mathbf{x}_{\mathbf{V}}(t)$  in the platelet's moving neighborhood volume  $\delta \mathbf{V}$ , the total rate of stress change,  $d\sigma_{mn}(\mathbf{x}_{\mathbf{V}},t)/dt$  is given by:

$$d\sigma_{mn}(\mathbf{x}_{\mathbf{V}},t)/dt = \partial\sigma_{mn}(\mathbf{x}_{\mathbf{V}},t)/\partial t + d\mathbf{x}_{\mathbf{V}}(t)/dt \partial\sigma_{mn}(\mathbf{x}_{\mathbf{V}},t)/\partial \mathbf{x}_{\mathbf{V}}(t)$$
(14)

However, this not a full description of the total stress rate since as remarked above the state of stress is a functional of the current hydride-crack length  $\mathbf{b}_2(t)$ , which is the time integral of the hydride growth velocity attribute  $\mathbf{b}_2$ . Thus, the stress tensor  $\sigma_{mn}$  written as functional of the current hydride-crack length  $\mathbf{b}_2(t)$ , is denoted by  $\sigma_{mn}(\mathbf{x}_{\mathbf{V}},t;\mathbf{b}_2(t))$ , and its time derivative is:

$$d\sigma_{mn}(\mathbf{x}_{\mathbf{V}},t; \mathbf{b}_{2}(t))/dt = \partial \sigma_{mn}(\mathbf{x}_{\mathbf{V}},t; \mathbf{b}_{2}(t))/\partial t + d\mathbf{b}_{2}(t)/dt \partial \sigma_{mn}(\mathbf{x}_{\mathbf{V}},t; \mathbf{b}_{2}(t))/\partial \mathbf{b}_{2}(t) + d\mathbf{x}_{\mathbf{V}}(t)/dt \partial \sigma_{mn}(\mathbf{x}_{\mathbf{V}},t; \mathbf{b}_{2}(t))/\partial \mathbf{x}_{\mathbf{V}}(t)$$

$$(15)$$

This total rate of stress, as well as a similar total rate for temperature (but no  $b_2$  rate term), has all the correct terms that should be evaluated in assessing the hydride growth velocity of Eq (10) in conjunction with Eq (13), since the moving neighborhood volume  $\delta V$  would be moving such that platelet growth velocity  $b_2 n_2$  is equal to  $dx_V(t)/dt$ . Using this equality for this analysis, and neglecting a similar term for the temperature rate, Eq(10) becomes functionally:

$$b_{2}(\mathbf{n}_{2} + \Delta[\mathsf{H}_{eq}(\mathbf{x}_{V},t)]/\Delta\sigma_{mn}(\partial\sigma_{mn}(\mathbf{x}_{V},t; \mathbf{b}_{2}(t))/\partial\mathbf{b}_{2}(t) + \partial\sigma_{mn}(\mathbf{x}_{V},t; \mathbf{b}_{2}(t))/\partial\mathbf{x}_{V2}(t)) \delta\mathbf{V}^{\bullet}) =$$

$$(x[Zr]\mathbf{A}_{2}\mathbf{n}_{2})^{-1}((\Lambda_{*}\mathbf{n}[\mathsf{H}(\mathbf{x}_{A},t,\Lambda)]) \underline{\mathbf{A}}_{2}\mathbf{n}_{2} - (\Delta[\mathsf{H}_{eq}(\mathbf{x}_{V},t)]/\Delta\mathsf{T}(\mathbf{x}_{V},t) d\mathsf{T}(\mathbf{x}_{V},t)/dt$$

$$+ \Delta[\mathsf{H}_{eq}(\mathbf{x}_{V},t)]/\Delta\sigma_{mn} \partial\sigma_{mn}(\mathbf{x}_{V},t; \mathbf{b}_{2}(t))/\partial t)\delta\mathbf{V})$$

$$(16)$$

In Eq (16),  $\delta V^{\bullet}$  is defined as  $(x[Zr]\mathbf{A_2n_2})^{-1}$   $\delta V$ , and the hydride-crack velocity instability is due to the possibility that the coefficient

### **Summary**

An assessment of safety, design, and cost tradeoff issues for short (ten to fifty years) and longer (fifty to hundreds of years) interim dry storage of spent nuclear fuel in Zircaloy rods shall address potential failures of the Zircaloy cladding caused by the precipitation response of zirconium hydride platelets. To perform such assessment analyses rigorously and conservatively will be necessarily complex and difficult. For

Zircaloy cladding, a model for zirhydride induced crack propagation velocity was developed for a decreasing temperature field and for hydrogen, temperature, and stress dependent diffusive transport of hydrogen to a generic hydride platelet at a crack tip. The development of the quasi-steady model is based on extensions of existing models for hydride precipitation kinetics [2] for an isolated hydride platelet at a crack tip. An instability analysis model of hydride-crack growth was developed using existing concepts in a kinematic equation for crack propagation at a constant thermodynamic crack potential subject to brittle fracture conditions [9]. At the time an instability is initiated, the crack propagation is no longer limited by hydride growth rate kinetics, but is then limited by stress rates. The model for slow hydride-crack growth will be further evaluated using existing available data such as that found in references [1, 3, 4, 5, 6, 10, 11, 16, 17].

This work was performed under the auspices of the U.S. Department of Energy by University of California Lawrence Livermore National Laboratory under contract No. W-7405-Eng-48.(UCRL-JC-141061).

### References

- [1]. Sawatzky, A. and C.E. Ells, *Understanding Hydrogen in Zirconium*, Zirconium in the Nuclear Industry (12<sup>th</sup> Symposium), ASTM STP1354, pp32-48, 2000.
- [2]. Stout, R.B., *Deformation and Thermodynamic Model for Hydride Precipitation Kinetics in Spent Fuel Cladding*, Lawrence Livermore National Rpt. UCRL-100860, October 1989.
- [3]. Dutton, R., K. Nuttal, M.P. Puls, and L.A. Simpson, *Mechanism of Hydrogen Induced Delayed Cracking in Hydride Forming Metals*, Metallurgical Transactions A, **8A**, pp1553-1562, Oct, 1977.
- [4]. Simpson, L.A., and M.P. Puls, *Effects of Stress, Temperature, and Hydrogen Content on Hydride-Induced Crack Growth in Zr-2.5Pct Nb,* Metallurgical Trans. A, **10A**, pp1093-1105, 1979.
- [5]. McMinn, A., E.C.Darby, and J.S. Schofield, *The Terminal Solid Solubility of Hydrogen in Zirconium Alloys,* Zirconium in the Nuclear Industry (12<sup>th</sup> Symp.), STP1354, pp178-195, 2000.
- [6]. Kammenzind, B.F., B.M. Berquist, R. Bajaj, P.H. Kreyns, and D.G. Franklin, *The Long Range Migration of Hydrogen Through Zircaloy in Response to Tensile and Compressive Stress Gradients*, Zirconium in the Nuclear Industry (12<sup>th</sup> Symp.), STP1354, pp196-233, 2000.
- [7]. Clayton, J.C., *Internal Hydriding in Irradiated Defected Zircaloy Fuel Rods- A Review*, Westinghouse Electric Corp. Rpt.-BAPL-WAPD-TM-1604, 1987.
- [8]. Stout, R.B., and H.R. Leider, editors, *Waste Form Characteristics Report, Revision-1*, Lawrence Livermore National Rpt. UCRL-ID-108314, November 1997.
- [9]. Stout, R.B., *Deformation and Thermodynamic Response for a Dislocation Model of Brittle Fracture*, J. of Eng. Fract. Mech., **19**, pp545-570, 1984.
- [10]. Eadie, R.L. and F. Ellyin, *The Effect of Hydride Precipitation on the Stresses near the Crack Tip in a Delayed Hydride Crack in Zirconium-2.5% Nb*, Scripta Metallurgica, **23**, pp585-592, 1989.
- [11]. Mueller, W.M., J.P. Blackledge, and G.G. Libowitz, editors, <u>METAL HYDRIDES</u>, Chapter 7, *Zirconium Hydrides and Hafnium Hydrides*, R.L. Beck and W.M. Mueller, Academic Press, 1968.
- [12]. Stout, R.B., *Discontinuum Mechanics and Dislocation Dependent Displacement Compatibility Equations*, Lawrence Livermore National report in preparation UCRL-JC- xxxx, December, 2000.
- [13]. Oriani, R.A., *Thermomigration in Solid Metals*, J. Phys. Chem. Solids, <u>30</u>, pp339-351, 1969. [14]. Marino, G.P., *HYDIZ-A 2-Dimensional Computer Program for Migration of Interstitial Solutes in Hydride Forming Metals*, Westinghouse Electric Corp. Rpt.-BAPL-WAPD-TM-1157, 1974.
- [15]. Nolfi, F.V., Thermodynamic driving forces for shape changes and diffusion in nonhydrostatically stressed solids, J. Appl. Phys., **44**, pp5245-5253, 1973.
- [16]. Lufrano, J., P. Sofranis, and H.K. Birnbaum, *Modeling of Hydrogen Transport and Elastically Accommodated Hydride-Formation near a Crack Tip*, J. Mech. Phys. Solids, <u>44</u>, pp179-205, 1996.
- [17]. Shek, G.K., M.T. Jovanovic, H. Seahra, Y. Ma, D. Li, and R.L. Eadie, *Hydride morphology and striation formation during delayed hydride cracking in Zr-2.5% Nb*, J. Nucl. Mat'ls, **231**, pp221-230, 1996.